



Study on the Linear Buckling Behaviour of Two Local Bamboo Species Under Different Length and Boundary Conditions via Finite Element Analysis (FEA)

Hazrina Mansor¹(✉), Mohammad Rosnizam Lop², and Buan Anshari³

¹ School of Civil Engineering, College of Engineering, Universiti Teknologi MARA (UiTM), Shah Alam, Malaysia

hazrina4476@uitm.edu.my

² Mohammad Rosnizam Lop School of Civil Engineering, College of Engineering, Universiti Teknologi MARA (UiTM), Shah Alam, Malaysia

³ Department of Civil Engineering, Faculty of Engineering, University of Mataram, Mataram, Indonesia

buan.anshari@unram.ac.id

Abstract. Bamboo is the world's fastest-growing grass species. Although bamboo is a resilient and sustainable engineering material, its use in the building sector has been limited. The limitation in the usage is most likely due to its nature, which might vary depending on the species and origin, creating a challenge in establishing standard design guidelines. As a result, further research into the fundamentals of bamboo as a structural material is required. The Finite Element (FE) method is used in this study to evaluate the elastic critical buckling loads and mode shape of two local bamboos under different lengths and boundary conditions. The proposed local bamboo was modelled in ABAQUS software version 6.14. The findings reveal that *Dendrocalamus asper* has greater buckling strength due to its physical dimensions than *Bambusa vulgaris* under the same length and boundary condition. In terms of length and boundary conditions, six-meter length bamboo with fixed-pinned ended conditions can resist higher elastic critical buckling load than six-meter bamboo with fixed-free ended conditions. Consequently, the difference in elastic critical buckling load between the finite element approach and Euler's theory calculation is less than 2%, indicating that the two methods are in good agreement.

Keywords: *Dendrocalamus asper* · *bambusa vulgaris* · elastic critical buckling load · Finite Element Analysis · Linear buckling analysis

1 Introduction

Bamboo has been used in construction for decades but only for minor projects. Until the 1980s, its use was limited to scaffolding and modest dwellings. Consequently, due to a lack of guidelines and standards for applying bamboo, its usage is limited, particularly

in construction [1–4]. In addition, much past research has reported that bamboo has a range of distinct characteristics that vary according to species, origin, position on bamboo culm, and maturity, making it more challenging to design as a structural element [5–8].

In terms of bamboo origin, each country has natural features that vary according to the weather and climatic conditions. Such conditions can affect the growth of bamboo. In other words, origins and sources produce varieties of bamboo species with different characteristics. At least over 1500 species of bamboo have been identified and explored around the world [9]. In general, there are ten types of the bamboo genus, and they are further divided into fifty-nine (59) species, in which thirty-nine (39) out of fifty-nine (59) are local species. In Malaysia, bamboo species are locally found in Sarawak (45%), Sabah (24%) and 31 percent (31%) in Peninsula Malaysia. *Gigantochloa levis* (Buluh Beting), *Schizostachyum grande* (Buluh Semeliang), *Gigantochloa wrayi* (Buluh Beti), *Dendrocalamus asper* (Buluh betung), *Gigantochloa scortechinii* (Buluh Semantan) and *Schizostachyum zollingeri* (Buluh Dinding) are the existing Malaysian bamboo resources [10]. A shortlist of five relevant species have been identified, namely *Gigantochloa wrayi* (Buluh Beti), *Gigantechloa scortechinii* (Buluh Semantan), *Gigantochloa levis* (Buluh Beting), *Gigantochloa atroviolacea* (Buluh Hitam) and *Dendrocalamus asper* (Buluh Betong) as the potential species under the forest plantation development program in Malaysia. Four species (i.e. *Dendrocalamus asper* (Buluh Betong), *Gigantochloa atroviolacea* (Buluh Hitam), *Gigantochloa levis* (Buluh Beting) and *Gigantechloa scortechinii* (Buluh Semantan)) have been previously used for the construction industry [10]. Each species has different culm height and geometrical characteristics, such as external and internal diameter, culm thickness, and skin colour [7]. *Schizostachyum grande* has the highest culm height at 32 m. In contrast, *Bambusa vulgaris* and *Bambusa blumeana* have the lowest height at 16 m. (N. Siam et al., 2019) [7].

Bambusa pervariabilis (Kao Jue) and *Phyllostachys pubescens* (Mao Jue) are bamboo species often used in construction in Hong Kong and Southern China. Both species exhibit different physical properties in terms of culm diameter. Research in [11] conducted by Chung et al. (2002), stated that the outer diameter for Kao Jue is relatively standardized and uniform over the length, with a 45 mm average. In contrast, the outer diameter of Mao Jue gradually reduces from roughly 80 mm to 50 mm, as does the height of the culm from the bottom to the top. It may be observed that there are variations in the physical characteristics of bamboo not only between different species but also within the same species. For instance, *Phyllostachys Viridiglaucescens* species in Italy have been collected from two different places and show different skin tones. The bamboo from the forest in Lucca is coloured between ochre to brown, while greenish bamboo originated in Roma [12].

Chung and Yu, 2001 reported that the position of the bamboo culm also plays a significant role in the mechanical properties of bamboo [13]. For *Kao Jue* and *Mao Jue*, the dry density is found uniformly distributed along the culm with an average value of 700 kg/m³. At the same time, the moisture content for *Kao Jue* is slightly fair at 12.5%, but a large variety of moisture content for *Mao Jue* is within 40% at the bottom and 20% at the top of the culm [13]. This is due to the gradual change in the diameter of *Mao Jue* bamboo along the culm. In addition, the study review by Ming et al. in [14] shows that the fibre density rises from the bamboo's lower part to the upper part. The nodes

section divides the internode and helps strengthen the bending force when the bamboo bends. Virtually, the length of the internodes varies at each bottom, middle, and top part of the bamboo culm. The bamboo's internode length rises from the base to the middle and then falls as it approaches the summit. For most bamboo species, the thickness and cross-sectional area decrease from the bottom to the top [14].

According to Raj and Agarwal (2014) [15], bamboo is acceptable for use in a building when it is 3–6 years old, whereas 6–9 months old bamboo is only suitable for basket handicrafts. On average, bamboo will gradually lose its advantages when it has reached more than 6 years of age [15]. Research conducted by [16] highlighted that the fibrous content affects the growth and strength of bamboo. The comparison between two generations of *Kao Jue* and *Mao Jue* species by T. Lo et al., (2008) [16] shows that the old bamboo gives a higher average number of vascular bundles of sclerenchyma fibre in bamboo, contributing to higher density. In addition, for old bamboo, *Mao Jue* has the greatest average number of vascular bundles with a maximum value of 10.75 compared to *Kao Jue*, with only 5.87. This means that the amount of fibres in bamboo differs at every age and species.

Awaluddin et al. [17] reported that the mean compressive strength of bamboo was higher at the top, followed by the middle and bottom parts of the bamboo culm. The result reported in [17] is supported by N. Daud et al. (2018) in [18]. For both treated and untreated, the top portion of *Gigantochloa scortechinii* showed the maximum compressive strength due to the substantial thickness of the bamboo wall and high cross-sectional area compared to the middle and bottom sections. The end bearing failure occurs in the higher thickness part of the culm, while the lower thickness part will be faced with splitting failure. Nonetheless, if the bamboo is allowed to dry for a period of time, the compressive strength of the bamboo can be increased in proportion to the reduction in moisture content [17]. Meanwhile, the tensile strength resistance of bamboo is governed by the composition of the bamboo, which consists of thin-walled cell-matrix and thick-walled fibre cells. The thin-wall cell matrix is a function to connect and transfer the load, while the thick-wall cells play the role of load-bearing [19]. According to Liu et al., 2020 in [19], the internode segment contributes significantly to the tensile strength resistance. The longitudinal tensile strength of the internode segment is 1.28 times that of the nodal section. However, in transverse tensile strength, the nodal section is higher than the internode section. It indicates that the node along the bamboo culm acted as a joint, contributing to the tensile strength.

The study reported in [20] highlighted that it is likely to have misleading conclusions from some widely available published data on bamboo strength as the strength and characteristics vary from species to species. In some of the studies, an apparent nonlinear softening behaviour up to failure was reported beyond the elastic limit [20, 21]. In contrast, studies reported in [22–24] do not show evidence of any significant ductility beyond the elastic limit. To understand how different species affect the behaviour of the bamboo pole, it is essential to take a step back and investigate the elastic behaviour of the bamboo pole for different species. Determination of the elastic critical buckling load is crucial as it is the basis fundamental in designing column. Therefore, this paper focuses on assessing the elastic linear buckling behaviour of two species of bamboo, namely *Dendracalamus asper* and *Bambusa vulgaris* to contribute to the insight of the

buckling behaviour of these two species via finite element method. In [6], a comparison of buckling strength between 3 species commercially utilized shows that *Dendrocalamus asper* has the highest buckling strength compared to *Bambusa vulgaris* and *Gigantochloa scortechinii*. This study aims to determine whether any outcomes from the elastic stage behaviour are misleading and develop the basis FEA modelling technique in analyzing bamboo material. The majority of past research has used experimental work to examine bamboo behaviour. Since experimental work can be time-consuming, this study will predict the accuracy of FEA in evaluating bamboo behaviour. Only elastic linear buckling analysis was carried out, and the precision of the results was compared with the Euler's theory.

1.1 Selection of Bamboo Species

Many bamboo species in Peninsular Malaysia belong to multiple genera, including *Bambusa*, *Dendrocalamus*, *Schizostachyum*, *Gigantochloa*, *Thyrsostachys*, *Dinochloa*, and *Racemobamboos*. In this work, two (2) common bamboo species were selected, namely *Bambusa vulgaris* (Fig. 1) and *Dendrocalamus asper* (Fig. 2). The two species of bamboo were chosen from two different genera and based on the availability of data. The geometrical dimensions of the *Bambusa vulgaris* and *Dendrocalamus asper* utilized in this investigation are shown in Table 1. The magnitude of this dimension has been derived from previous research results taken from [6, 7]. N. Siam et al. (2019) investigated thirteen local bamboos' anatomical, physical, and mechanical aspects, which provide critical information and data, particularly the dimensions of local bamboo.



Fig. 1. *Bambusa vulgaris* [10].



Fig. 2. *Dendrocalamus asper* [10].

Table 1. Dimension Of The Proposed Bamboo Pole.

Species	The physical characteristic of the proposed bamboo			
	Length (m)	Internode length (mm)	External diameter (mm)	Culm thickness (mm)
<i>Bambusa Vulgaris</i> ^a	6, 9, 12	330	95	9
<i>Dendracolumus Asper</i> ^b	6, 9, 12	370	102	16

^a Known as Buluh Minyak, ^b Known as Buluh Betong

Three distinct bamboo pole lengths—6 m, 9 m, and 12 m for each species- were modelled in the Abaqus FEA. The bamboo lengths used in this study were chosen randomly to compare and analyze the influence of length on the buckling behaviour of the two local bamboos. Detail of the six (6) bamboo specimens included in this study can be referred to in Table 1. Each bamboo pole is evaluated with two (2) different boundary conditions. The first boundary condition is the fixed-pinned support, where the fixed support is assigned at the bottom, and pinned support is assigned at the top of the bamboo. All the degrees of freedom about the rotational and translational movements are restrained for the fixed end. Instead, the pinned end allowed the structure of the bamboo pole to rotate, but only the translational movement in the vertical direction was allowed. The third condition has been set as a fixed-free support system. The upper side of the bamboo poles will be free without any restrained support.

1.2 Theoretical Calculation

For the theoretical calculation, the established Euler’s buckling theory formula is applied to calculate the critical buckling load for a long column. According to Euler’s theory, the critical buckling load is the ultimate load it can resist when a column is on the edge of buckling. Euler’s theory formula is

$$P_{cr} = \frac{\pi^2 EI}{L_{eff}^2} \quad (1)$$

Where; E = Young’s modulus of column material, I = Area moment of inertia, and Leff = Effective length of the column.

The column end condition may contribute to determining the effective column length, Leff. The effective length factor, K, is used to connect columns that have different end conditions. Fig. 3 shows the value of the theoretical effective length factor based on different end conditions. The effective length of a column is the same as that of an analogous pinned-pinned column. It can be computed as follows:

$$L_{eff} = \text{Length factor, } K \times \text{Actual length, } L \quad (2)$$

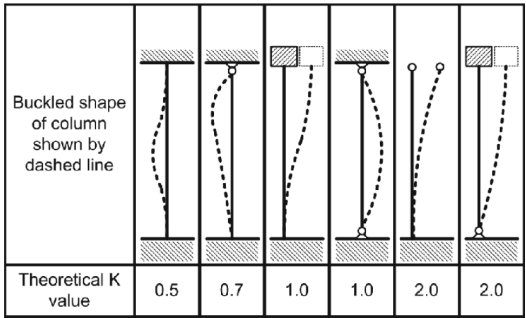


Fig. 3. The value of theoretical effective length factor, K

Table 2. Material properties for bamboo species.

Species	Mechanical Properties of the proposed bamboo				
	Density (kg/m^3)	Young's Modulus (N/mm^2)	Moisture Content (%)	Modulus of Rupture (MOR) (N/mm)	Poisson's Ratio
<i>Bambusa Vulgaris</i> ^a	610	12104	12	172	0.45
<i>Dendracolumus Asper</i> ^b	559	11303	12	150	0.45

^a Known as Buluh Minyak, ^b Known as Buluh Betong

2 Finite Element Model of the Bamboo Pole

The finite element analysis method is used to achieve the study’s objectives. The proposed bamboo in Table 1, i.e. *Bambusa vulgaris* and *Dendrocalamus asper* was modelled in ABAQUS software. A 3-dimensional (3D) modelling space with deformable type was used. The base feature of solid extrusion is selected to model the bamboo pole. Each bamboo specimen consisted of three parts: a node, an internode, and an extra. The extra part is a bamboo internode that can be used to complete the desired length of bamboo. Two material behaviours: density and elasticity, were assigned. The elastic properties included are Young’s Modulus and Poisson’s ratio. The material properties are shown in Table 2.

Next, all the parts were assembled as an instance to complete the entire bamboo pole (refer to Fig. 4). A linear buckling analysis was selected to examine the critical buckling load and the linear elastic buckling mode shape of the proposed bamboo. In this study, two (2) types of boundary conditions have been created for all bamboo poles. First, the bamboo pole was fixed at one end using encastre ($U1, U2, U3, UR1, UR2$ and $UR3 = 0$) support, and the other end was assigned as ($U1, U3, UR1, UR2$ and $UR3 = 0$) for pinned support. Second, only one end side was set as fixed while free at the other end side.

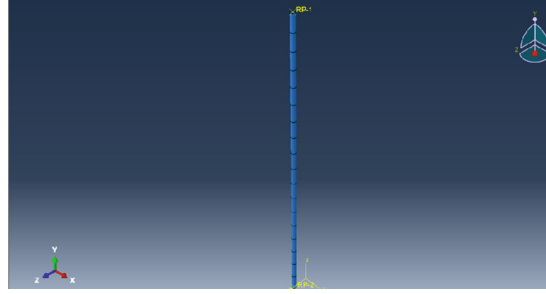


Fig. 4. Assemble instances of the bamboo pole.

A 50 N concentrated force was applied vertically downward to the top of the bamboo pole. A three-dimensional continuum eight-node reduce integration (C3D8R) element was used with an approximately global size of 10 mm seeds. Linear buckling analysis was carried out with the utilization of subspace eigensolver. The linear buckling analysis is a straightforward finite element analysis method. However, the results provided can be limited. Eigenvalue linear buckling analysis conducted in this study provides the elastic critical buckling load of the examined bamboo.

3 Results

The analysis results generated from the software were compared to the theoretical Euler buckling formula. The critical buckling load and mode shape for *Bambusa vulgaris* and *Dendrocalamus asper* under various length and boundary conditions was also presented.

3.1 Linear Buckling Analysis and Critical Buckling Load Comparison

Twelve bamboo specimens were modelled in Abaqus FEA software, with six specimens developed for each bamboo species. Each of the six (6) specimens was modelled with different lengths and boundary conditions. The critical buckling load for each bamboo specimen was determined employing the Eq. 3 as follows:

$$P_{cr}(N) = \text{eigenvalue} \times \text{applied load (N)} \quad (3)$$

The critical buckling loads resulting from Abaqus for both bamboo species under different lengths and boundary conditions were presented in Table 3. The critical buckling load is derived by multiplying the eigenvalue obtained from the buckling analysis with the 50 N applied load. The species *Dendrocalamus asper*, 6 m long with fixed-pinned boundary condition, has the greatest eigenvalue, which reaches 515. Consequently, it has led to the highest elastic critical buckling load of 25773 N. The results show that the elastic critical buckling load calculated from Euler's theory offers the same conclusion. The 6m long *Dendrocalamus asper* with fixed-pinned end condition yields the highest critical buckling load.

Table 3 illustrate almost identical results. For all cases, the elastic critical buckling load of *Dendrocalamus asper* is greater than the *Bambusa vulgaris* species. For example,

Table 3. Finite element analysis results for bamboo species.

Species	Boundary Condition	Length (mm)	Applied load (%)	Eigenvalue	Critical Buckling load, <i>Per</i> (N) (FEA)	Critical Buckling load, <i>Per</i> (N) (Euler Theory)	Buckling Stress, σ (N/mm ²) (FEA)	Buckling Stress, σ (N/mm ²) (Euler Theory)
<i>Bambusa Vulgaris</i> ^a	Fixed-pinned	6000	50	303	15139	15393	6.23	6.33
		9000	50	135	6736	6841	2.77	2.81
		12000	50	76	3790	3848	1.56	1.58
	Fixed-free	6000	50	38	1854	1885	0.76	0.78
		9000	50	16	824	838	0.34	0.34
		12000	50	9	463	471	0.19	0.19
<i>Dendrocalamus</i>	Fixed-pinned	6000	50	515	25773	26149	5.96	6.05
		9000	50	229	11463	11622	2.65	2.69
		12000	50	129	6449	6537	1.49	1.51

Species	Boundary Condition	Length (mm)	Applied load (%)	Eigenvalue	Critical Buckling load, <i>Per</i> (N) (FEA)	Critical Buckling load, <i>Per</i> (N) (Euler Theory)	Buckling Stress, σ (N/mm ²) (FEA)	Buckling Stress, σ (N/mm ²) (Euler Theory)
	Fixed-free	6000	50	63	3155	3203	0.73	0.74
		9000	50	28	1402	1424	0.32	0.33
		12000	50	16	789	801	0.18	0.19

^aKnown as Buluh Minyak, ^bKnown as Buluh Betong.

regardless type of species, the 6 m fixed-pinned end supported appear to have the highest buckling load value for their respective species.

3.2 Buckling Stress

The critical buckling stress is generally lower than the yield stress in slender columns. Buckling stress may be calculated theoretically using the following formulas (Eq. 4):

$$\sigma = F/A \tag{4}$$

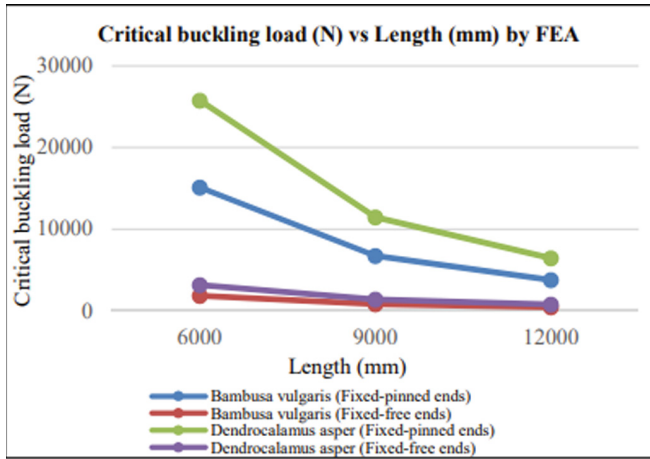


Fig. 5. The relationship between critical buckling load and bamboo length.

Where σ is buckling stress, F is buckling load, and A is the cross-sectional area of bamboo.

Each bamboo has its unique set of characteristics and physical properties, which influence the area of its cross-sections. According to this study, the two species tested had different areas, with *Bambusa vulgaris* having a cross-sectional area of 2431.59 mm^2 and *Dendrocalamus asper* having a cross-sectional area of 4322.83 mm^2 . The *Dendrocalamus asper* species has greater dimensions than the *Bambusa vulgaris*, with an outer diameter of 102 mm and an inner diameter of 70 mm, compared to 95 mm and 77 mm, respectively. The difference in cross-sectional area between these two bamboo species explains the significant difference in their buckling stress resistance.

The determined buckling stress for each FE bamboo model has a similar trend to the elastic critical buckling load. The 6 m with fixed-pinned ends bamboo encompassed the greatest value, with a value of 6.23 N/mm^2 for *Bambusa vulgaris* and 5.96 N/mm^2 for *Dendrocalamus asper*, which was confirmed by the Euler theoretical calculations with 6.33 N/mm^2 and 6.05 N/mm^2 for *Bambusa vulgaris* and *Dendrocalamus asper*, respectively. The value of the critical buckling load obtained using Euler's theory is slightly greater than that obtained from the Abaqus finite element analysis, with an overall difference of less than 2% for all cases.

Figure 7 depicts the correlations between the elastic critical buckling load obtained in Abaqus FE and Euler buckling formulation. As can be seen, the regression line yield the coefficients of determination, or R-squared value equal to 1, indicating that the bamboo model explains all of the variability of the collected data around its mean value. This implies that analyzing the buckling behaviour of bamboo utilizing software is successful and consistent with its theory. According to Euler's theory, the stress in a column caused by a direct load is minor compared to the stress caused by bending failure. This is because the specimen columns shall be entitled entirely straight with no flaws. However, a minor disparity may result from a systematized procedure in the Abaqus software (Fig. 6).

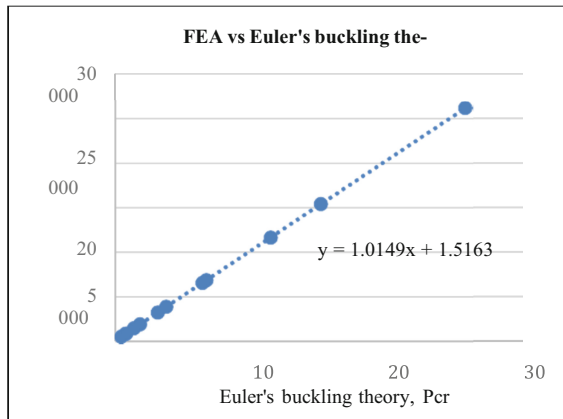


Fig. 6. Pcr Abaqus FEA vs Pcr Euler's theory.

3.3 Buckling Mode Shape

The form of the buckling mode can be interpreted by the shape of a structural column's failure following bending due to load. According to Euler's theory, the pinned end can be frictionless where there is no moment constraint. In contrast, the fixed end can be considered a rigid condition with no deflection due to the rotational. The boundary condition of the column itself has the most influence on the transformation towards the failure mode. For fixed-pinned end conditions, slender structures, especially these bamboo specimens, will experience curvature around the middle part of the structure. This is because each end has been constrained to allow horizontal translation movement. On the other hand, a curve will develop at the top of the structure where the end condition is free and not constrained by any support criteria. Example influence of fixed-free and fixed-pinned end conditions on the shape of the buckling mode for both bamboo species.

In this study, all fixed-pinned bamboo specimens and fixed-free specimens had the same reaction and responses that fit that description. Figure 8 shown serve as evidence to clearly show the buckling mode shape for each bamboo specimen. However, referring to the visualization of each bamboo specimen in finite element analysis, it appears that the buckling mode shape changes only between end support conditions, but it remains the same response regardless of the changes in length and bamboo species. For a more realistic perspective, Figs. 8, 9, 10, 11, 12 and 13 visually show the example influence of fixed-free and fixed-pinned end conditions on the shape of the buckling mode for both bamboo species.

3.4 Effect of Boundary Condition

According to the Abaqus software visualization, the bamboo structure tied to a fixed condition at the bottom end demonstrates that even though the bamboo structure changes due to buckling almost throughout the base, there remains no rotation at the end where it is fixed. Fixed end support will restrain translational movement towards vertical and horizontal forces and rotational due to the moment. On the other hand, pinned support

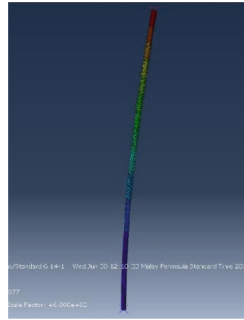


Fig. 7. *Bambusa vulgaris* (6 m, fixed-free ends)

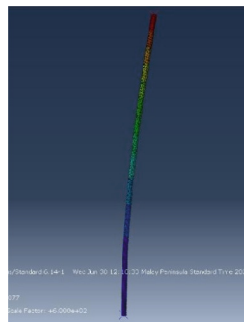


Fig. 8. *Bambusa vulgaris* (12 m, fixed-free ends).

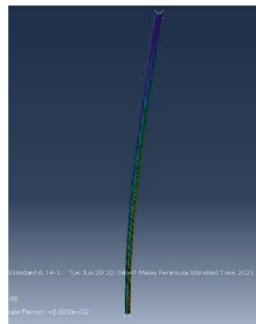


Fig. 9. *Dendrocalamus asper* (6 m, fixed-free ends)

will allow translational and rotational. In this case, pinned support is translationally restrained in both horizontal axes, which is x-axis and z-axis while allowing translation for y-axis. The rotation is allowed at all axes. It enables the bamboo column to bend from start from the end support. From the linear buckling analysis of bamboo, fixed-pinned bamboo specimens have greater elastic critical buckling loads than fixed-free specimens. This is because the constraints of each support have a distinct influence on the bamboo's

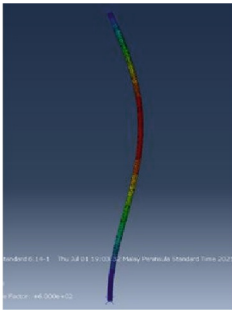


Fig. 10. *Bambusa vulgaris* (9 m, fixed-pinned ends).

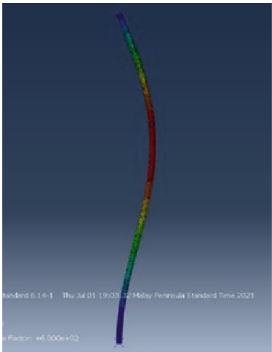


Fig. 11. *Bambusa vulgaris* (6 m, fixed-pinned ends)

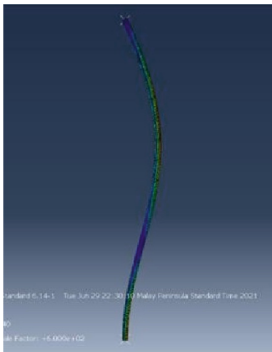


Fig. 12. *Dendrocalamus asper* (12 m, fixed-pinned ends)

strength, particularly in translation movement. It has been observed in both *Bambusa vulgaris* and *Dendrocalamus asper* bamboo species.

In terms of boundary conditions, the critical buckling load for fixed-pinned specimens appear to be almost ten times greater than those for fixed and free-supported

bamboo. The results are the same for both finite element methods and theoretical calculations. A structure with boundary conditions at both ends has the advantage of receiving more support, offering greater strength to the bamboo in supporting the load, regardless of the type of bamboo species. When both boundary conditions for the *Bambusa vulgaris* species are compared, the critical load values for the fixed-pinned conditions are 15139 N, 6736 N, and 3790.30 N, respectively. In contrast, the elastic critical buckling load calculated for the fixed-free condition are only 1853.85 N, 823.90 N, and 463.45 N. Figure 5 depict the correlation between the elastic critical buckling load and the length of the bamboo, respectively. Each condition for both bamboo species exhibited a relatively uniform decrease in the elastic critical buckling load corresponding to the increase in bamboo length. The 3-m difference in length results in an approximately 50% reduction in the critical buckling load.

3.5 Effect of Bamboo Pole Length and Species

This analysis proposed three possible lengths: 6 m, 9 m, and 12 m. It is modified with uniform differences to get results that are also consistently proportional. It is reached when, with a 3-m increase in specimen length, the critical buckling load is reduced by approximately 50%, regardless of whether it is *Bambusa vulgaris* or *Dendrocalamus asper*. The length of the structural members can be considered to have influenced the structure's load-carrying capacity. The buckling load of a column is reduced by increasing its span length. The slenderness ratio of a column member is critical to its mechanism of failure in compression. It is expressed as the fraction of column length to the radius of gyration of column cross-sectional area. The general formula for slenderness ratio is as shown in Eq. 5:

$$\lambda = \frac{L}{r} \quad (5)$$

where, λ is slenderness ratio, L is effective length of column, and r is radius of gyration of cross-sectional area.

The greater the slenderness ratio, the lower the elastic critical buckling load. On the other hand, a stocky column will most likely not encounter buckling failure due to its low slenderness ratio.

The radius of gyration is based on a geometric property of the material applied in the study. It defined the crosssectional area distribution in a column around its centroidal axis. According to this study, each bamboo species has different mechanical and physical properties, such as the diameter and thickness of the bamboo culm. This dimensional measure necessarily gives the result of the calculation of the gyration radius of its own. It directly becomes a variable factor in the slenderness ratio for each bamboo species, influencing the evaluation of the critical buckling load.

3.6 Role of Effective Length

The role of effective length is very closely related to boundary conditions. According to Euler's theory, the effective column length is the length of an analogous pin ended

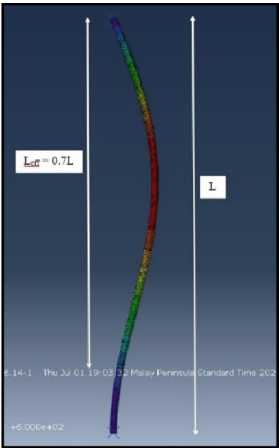


Fig. 13. Visualization for fixed-pinned ends

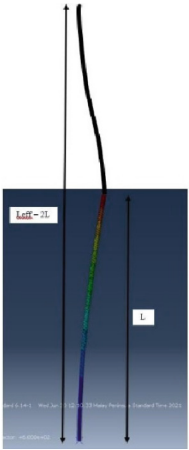


Fig. 14. Visualization for fixed-free ends.

column with the same load-carrying capacity as the member under evaluation. The lower a column's effective length, the less likely it is to buckle and the larger its weight bearing strength. The effective length should be referenced to the value of the coefficient factor according to the relevant boundary conditions for all other than pinned-pinned end columns. The effective length is the actual length where a buckling curve appears along the bamboo column when an axial force is applied. As shown in Fig. 13, the curve formed by compression of the fixed-pinned end bamboo was acceptable, as indicated in theory. There is no rotational movement at the fixed end, preventing curvature from end to end of the column. On the other hand, it differs visually from the buckling analysis of the fixed and free end conditions, illustrated in Fig. 14. Since there is no limitation at the top end, the imagined curve occurs at twice its original length.

4 Conclusions

The study uses the finite element method to study the elastic linear buckling analysis of local bamboo species. The two (2) bamboo species, *Bambusa vulgaris* and *Dendrocalamus asper*, were modelled in Abaqus software. The variation of bamboo species, length and boundary condition yield different values of elastic critical buckling load. The findings were verified by the theoretical calculations using Euler's column formula.

References

1. Janssen, J. J. A.: *Bamboo in Building Structure*. Ph.D. Thesis, Eindhoven University of Technology, The Netherland (1981).
2. Sun, X., et al.: Novel engineered wood and bamboo composites for structural applications: state-of-art of manufacturing technology and mechanical performance evaluation *Constr. Build. Mater.* (2020).
3. Liese, W.: Research on bamboo, *Wood Sci. Technol.* (21), 189–209 (1987).
4. Wu, W., Liu, Q., Zhu, Z., Shen, Y.: Managing bamboo for carbon sequestration, bamboo stem and bamboo shoots, *Small-Scale For.* 14 (2), 233–243 (2015). <https://doi.org/10.1007/s11842-014-9284-4>
5. Masdar, A., Suhendro, B., Siswosukarto, S., & Sulisty, D.: Determinant of Critical Distance of Bolt on Bamboo Connection. *Jurnal Teknologi*, 69(6) (2014). <https://doi.org/10.11113/jt.v69.3319>
6. Awalluddin, D., Azreen, M. A. M.: Hanim, O. M., Syahrizal, I. I., Warid, H. M.: Ismail, M. A., & Lee, H. S.: Interactive buckling of structural local bamboo in Malaysia. In *IOP Conference Series: Earth and Environmental Science*, Vol. 220, Institute of Physics Publishing (2019). <https://doi.org/10.1088/1755-1315/220/1/012036>
7. Abdullah, S. N., Uyup, M. K. A., Husain, H., Mohmod, A. L., and Awalludin, M. F.: Anatomical, physical, and mechanical properties of thirteen Malaysian bamboo species. *BioRes* 14(2), 3925–3943 (2019).
8. Dinie, A., et al.: *IOP CONFERENCE 2019, Ser.: Earth Environ Sci.* 220 012036 (2019).
9. Chung, K. F., and Yu, W. K.: Mechanical properties of structural bamboo for bamboo scaffoldings. *Eng. Struct.* 24, 429–442 (2002)
10. Baharuddin, N.: *Bengkel Penyediaan Tindakan Pembangunan Buluh Malaysia (2021–2030)*. Malaysian Timber Industry Board (MTIB) (2020).
11. Chung, K. F., & Yu, W. K.: Mechanical properties of structural bamboo for bamboo scaffoldings *Engineering Structures*. 24(4), 429–442 (2002). [https://doi.org/10.1016/S0141-296\(01\)00110-9](https://doi.org/10.1016/S0141-296(01)00110-9)
12. Fabiani, M.: Physical and mechanical properties of Italian bamboo culms. *CONFERENCE Paper of X World Bamboo Congress* (2015).
13. Chung, K.F., and Yu, W. K.: Full scale tests of Double Layered Bamboo Scaffoldings (DLBS). Technical Report, Research Centre for Advanced Technology in Structural Engineering, the Hong Kong Polytechnic University (2001).
14. Ming, Y. Thai. C., Jye, K. W., & Ahmad, I. A. H.: Mechanical properties of bamboo and bamboo composites: A Review. *Journal of Advanced Research in Materials Science* 35(1), 7–26 (2017). Retrieved from www.akademiabaru.com/arms.html.
15. Raj, D., & Agarwal, B.: Bamboo as a building material. *Journal of Civil Engineering and Environmental Technology* 1(3), 56–61 (2014). Retrieved from https://www.krishisanskriti.org/vol_image/03Jul201502074415.pdf

16. Lo, T. Y., Cui, H. Z., Tang, P. W. C., & Leung, H. C.: Strength analysis of bamboo by microscopic investigation of bamboo fibre. *Construction and Building Materials*, 22(7), 1532–1535 (2008). <https://doi.org/10.1016/j.conbuildmat.2007.03.031>
17. Awalluddin, D., Mohd, A. M. A., Osman, M. H., Hussin, M. W., Ismail, M. A., Lee, H. S., & Abdul, S. L. N. H.: Mechanical properties of different bamboo species. In *MATEC Web of CONFERENCES 2017*, Vol. 138, EDP Sciences (2017). <https://doi.org/10.1051/mateconf/201713801024>
18. Daud, N. M., Nor, N. M., Yusof, M. A., Al Bakhri, A. A. M., & Shaari, A. A.: The physical and mechanical properties of treated and untreated *Gigantochloa Scortechinii* bamboo. In *AIP Conference Proceedings*, Vol. 1930, American Institute of Physics Inc (2018). <https://doi.org/10.1063/1.5022910>
19. Liu, P., Zhou, Q., Jiang, N., Zhang, H., & Tian, J.: Fundamental research on tensile properties of phyllostachys bamboo. *Results in Materials*, 7, 100076 (2020). <https://doi.org/10.1016/j.rinma.2020.100076>
20. Lorenzo, R., Mimendi, L., Godina, M., Li, H.: Digital analysis of the geometric variability of Guadua, Moso and Oldhamii bamboo. *Constr. Build. Mater.* 236 117535 (2020). <https://doi.org/10.1016/j.conbuildmat.2019.117535>.
21. Ribeiro, R. A. S., Ribeiro, M.G. S., Miranda, I.P.A.: Bending strength and nondestructive evaluation of structural bamboo. *Constr. Build. Mater.* 146 , 38–42 (2017). <https://doi.org/10.1016/j.conbuildmat.2017.04.074>.
22. Lorenzo, R., Godina, M., Mimendi, L., Li, H.: Determination of the physical and mechanical properties of moso, guadua and oldhamii bamboo assisted by robotic fabrication. *J. Wood Sci.* 66(20) (2020). <https://doi.org/10.1186/s10086-020-01869-0>.
23. Shao, Z.P., Fang, C. H., Huang, S. X., Tian, G. L.: Tensile properties of Moso bamboo (*Phyllostachys pubescens*) and its components with respect to its fiber-reinforced composite structure. *Wood Sci. Technol.* 44 (4), 655–666 (2010). <https://doi.org/10.1007/s00226-009-0290-1>.
24. Dixon, P.G., Gibson, L.J.: The structure and mechanics of Moso bamboo material. *J. R. Soc. Interface.* 11 (99) 20140321 (2014). <https://doi.org/10.1098/rsif.2014.0321>.

Open Access This chapter is licensed under the terms of the Creative Commons Attribution-NonCommercial 4.0 International License (<http://creativecommons.org/licenses/by-nc/4.0/>), which permits any noncommercial use, sharing, adaptation, distribution and reproduction in any medium or format, as long as you give appropriate credit to the original author(s) and the source, provide a link to the Creative Commons license and indicate if changes were made.

The images or other third party material in this chapter are included in the chapter's Creative Commons license, unless indicated otherwise in a credit line to the material. If material is not included in the chapter's Creative Commons license and your intended use is not permitted by statutory regulation or exceeds the permitted use, you will need to obtain permission directly from the copyright holder.

